

Luminous flame around burning aluminum particle near burning surface of composite propellant – Numerical experiments in CO₂ and H₂O –

Kenichi Takahashi^{*†}, Rieko Doi^{*}, Takuo Kuwahara^{*}, and Toru Shimada^{**}

^{*}College of Science and Technology, Nihon University
7-24-1 Narashinodai, Funabashi, Chiba 274-8501, JAPAN
Phone : +81-47-469-5402

[†]Corresponding author : takahasi@aero.cst.nihon-u.ac.jp

^{**}Institute of Space and Astronautical Science, Japan Aerospace Exploration Agency
3-1-1 Yoshinodai, Chuo, Sagami-hara, Kanagawa 252-5210, JAPAN

Received : November 19, 2014 Accepted : March 13, 2015

Abstract

We conducted a three-dimensional numerical experiment to ascertain the luminous flame shape around a burning aluminum particle near the burning surface of composite propellant. To simulate the luminous flame around the burning aluminum particle, we incorporated vaporized aluminum ejected from the particle surface and simulated the decomposed gas flow around the particle. Results of numerical experiments show that the cloud of vaporized aluminum ejected from the aluminum particle surface spread around the particle. The cloud shape was streamlined, resembling a raindrop. The cloud shape changed by the gas velocity and the vaporized aluminum velocity. The cloud area decreased with increasing gas velocity and vaporized aluminum velocity. The numerically estimated luminous flame diameters are slightly smaller than the experimentally obtained results of our previous works.

Keywords : numerical experiment, three-dimensional, burning aluminum particle, vaporized aluminum, luminous flame

1. Introduction

Aluminum particles are used as an ingredient in composite propellants for solid rockets to improve the propellant performance. Almost all the aluminum particles agglomerate on the burning surface of the composite propellant. The particles ignite immediately and leave the burning surface^{1), 2)}. The decomposed gas flow and temperature profile near the burning surface affect the composite propellant performance^{3), 4)}. Therefore, investigating details of the aluminum particle behavior is important because the aluminum particles agglomerate and ignite near the burning surface^{5)–8)}. Near the burning surface, the agglomerated aluminum particles influence the decomposed gas flow. The burning aluminum particles there influence the temperature profile. The aluminum particles combust in gas phase, producing luminous flames around the particles^{9), 10)}. High temperatures occur there, affecting the temperature profile near the burning surface.

To clarify the effects of the burning aluminum particles on the temperature profile near the burning surface, it is important to investigate the shape of the luminous flame around the burning aluminum particle.

Many studies have investigated aluminum combustion over many years. These great works have revealed important information related to aluminum agglomeration, aluminum combustion, combustion products, etc.^{1), 2), 11), 12)}. In recent years especially, numerical approaches have been developed. These works provide much information about burning time, combustion products around aluminum particles, etc.^{13)–16)}. However, almost all works of numerical simulation have been performed in one or two-dimensions. Furthermore, few reports have described luminous flames around burning aluminum particles with numerical simulation.

For this study, we strove to ascertain the luminous flame shape around the burning aluminum particle near

the burning surface of the composite propellant using three-dimensional numerical experiments. To simulate the luminous flame around the burning aluminum particle, we examined vaporized aluminum ejected from the particle surface and simulated the decomposed gas flow surrounding the particle. We investigated the concentration distribution of the vaporized aluminum and estimated the luminous flame shape around the burning aluminum particle.

2. Numerical experiments

A model of the burning aluminum particle is presented in Figure 1. This model bases on our previous works^{5)–8)}, and it is simplified for the numerical experiment. Agglomerated aluminum particles melt on the burning surface of the composite propellant. Then, the agglomerated aluminum particle ignites and leaves the burning surface. After the vaporized aluminum is ejected from the melted aluminum surface, it wraps over the melted aluminum, forming a cloud. A reaction zone appears around the vaporized aluminum cloud. The luminous flame appears at the reaction zone. A small amount of alumina contained in aluminum particle melt and made an alumina cap on the melted aluminum. At the reaction zone an alumina is produced by reacting with the oxidizer. The alumina made an alumina tail at downstream of the burning aluminum particle.

Using numerical experiments, we elucidated the shape of the vaporized aluminum cloud around just ignited aluminum particle near the burning surface. OpenFOAM (A free, open source CFD software package; OpenCFD Ltd.) was used for numerical experiments, which were conducted using three-dimensional finite volume method. The solver was “reactionFoam” included in OpenFOAM. In this study, chemical reactions and turbulence models including this solver were not used. Open source software for pre-processing and post-processing (SALOME; Open CASCADE) was used for domain and mesh generation. The mesh was a non-structured mesh of tetrahedra.

Numerical experiments were conducted in a cylindrical domain as shown in Figure 2. The aluminum particle ignites immediately and leaves the burning surface. Therefore, the aluminum particle location was set to $1.5 D$

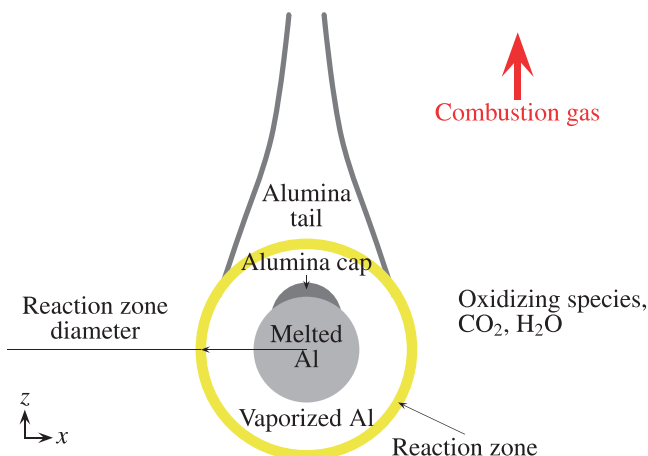


Figure 1 Model of burning aluminum particle.

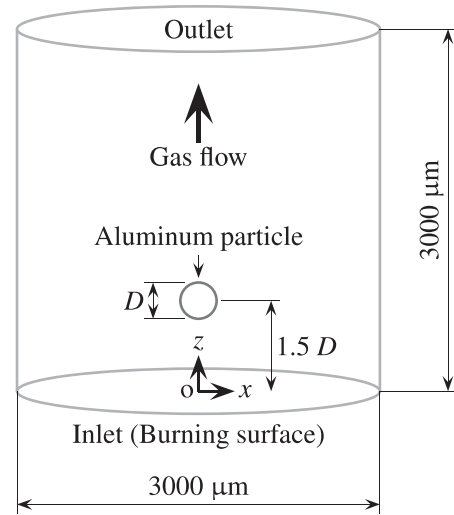


Figure 2 Computational domain of numerical experiments.

from the burning surface, where D is the aluminum particle diameter. The coordinate system is shown in Figure 2. The burning surface is set at the inlet face of the computational domain.

The initial and inlet conditions were obtained from the results of combustion experiments and theoretical calculations of our previous works^{5)–8)}. The gas temperature was set to the aluminum melting point²⁾. To simulate the heterogeneous decomposed gas velocity, the gas velocity was varied. The main oxidizers of the aluminum particles in the composite propellant were CO_2 and H_2O . These were used as the working fluid.

The aluminum particle diameter was set based on experimentally obtained results from our previous works^{5)–8)}. The burning aluminum particle was assumed as a spherical heat source. The aluminum particle surface temperature was referred from previous work²⁾. Furthermore, vaporized aluminum was ejected from the aluminum particle surface. The velocity of the vaporized aluminum ejected from the surface of the aluminum particle was calculated theoretically from the burning time of previous work¹¹⁾. To investigate the effect of the aluminum particle surface conditions, the vaporized aluminum velocity was varied.

As previously explained, to compare the experimental results, the computational conditions were set from our previous works^{5)–8)} and other previous works^{2), 11)}. The computational conditions of the numerical experiments are presented in Table 1. Table 2 shows the model of composite propellant for theoretical calculations. The composite propellant composition is the same as that used in our previous works^{5)–8)}.

3. Results and discussion

3.1 Concentration distribution of vaporized aluminum

The concentration distributions of vaporized aluminum around the aluminum particles are presented in Figures 3 and 4 for the respective working fluids and the particle diameters. The figures are cross-section views of the computational domain. The gas flow is in an upward direction of the figure. The green areas are the vaporized

Table 1 Computational conditions of numerical experiments.

Initial and inlet conditions	Laminar flow
	Velocity : $U_g = 7, 14 \text{ m s}^{-1}$ Temperature : $T_g = 1000 \text{ K}$
Working fluid	$\text{CO}_2, \text{H}_2\text{O}$
Aluminum particle	Spherical particle
	Diameter : $D = 100, 200, 300 \mu\text{m}$
	Vaporized Al velocity : $U_{Al} = 13.5, 6.8, 4.6 \text{ m s}^{-1}$
	Varied U_{Al} : $U_{Al} = 3.4, 6.8, 13.6 \text{ m s}^{-1}$ Surface Temperature : $T_{Al} = 3000 \text{ K}$

Table 2 Composition of composite propellant.

Ingredients	Composition [parts]	
Ammonium perchlorate, AP	NH_4ClO_4	80
Ammonium nitrate, AN	NH_4NO_3	10
Octadecyl alcohol, Oct	$\text{C}_{18}\text{H}_{38}\text{O}$	10
Aluminum, Al	Al	10

aluminum clouds mainly. The vaporized aluminum concentration in the cloud is about 30-70%. The concentration increases with proximity to the aluminum particle.

The vaporized aluminum clouds appear around the aluminum particles. The cloud shape is streamlined, resembling a raindrop. The streamlined shape is influenced and produced by the gas flow around the aluminum particle. The cloud shape is changed by the particle diameter. Therefore, it is considered that Reynolds number influences the cloud shape.

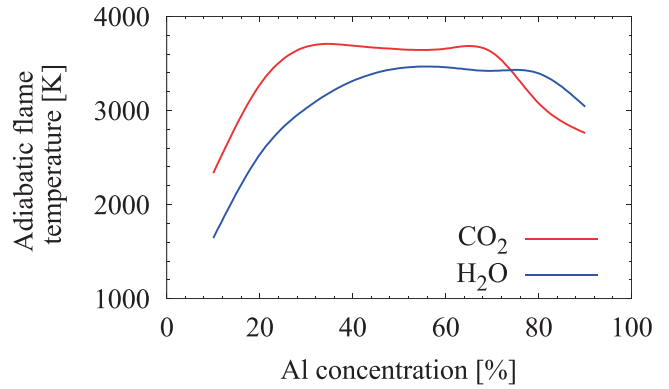


Figure 5 Mixing ratio of aluminum and oxidizer.

To estimate the luminous flame diameter of the aluminum particle, theoretically, we find the location of the reaction zone where the luminous flame appears. The ratio of the aluminum and the oxidizer is stoichiometric at the reaction zone. There, the temperature of the reaction of the aluminum and the oxidizer become the highest. To find the stoichiometric mixing ratio of the aluminum and the oxidizer, we conducted theoretical calculations of the mixtures of Al/CO_2 and $\text{Al}/\text{H}_2\text{O}$ with NASA CEA¹⁷⁾. The results are presented in Figure 5. The figure indicates the adiabatic flame temperature with changing aluminum concentration.

For CO_2 , the high temperature is about 30-70% of the concentration of aluminum. In the case of H_2O , it is about 50-80%. Consequently, we chose the median concentration in the high temperature region. We defined that the location of the reaction zone is set to 50% in CO_2 and 60% in H_2O of the concentration of aluminum.

The estimated diameters of the reaction zone are

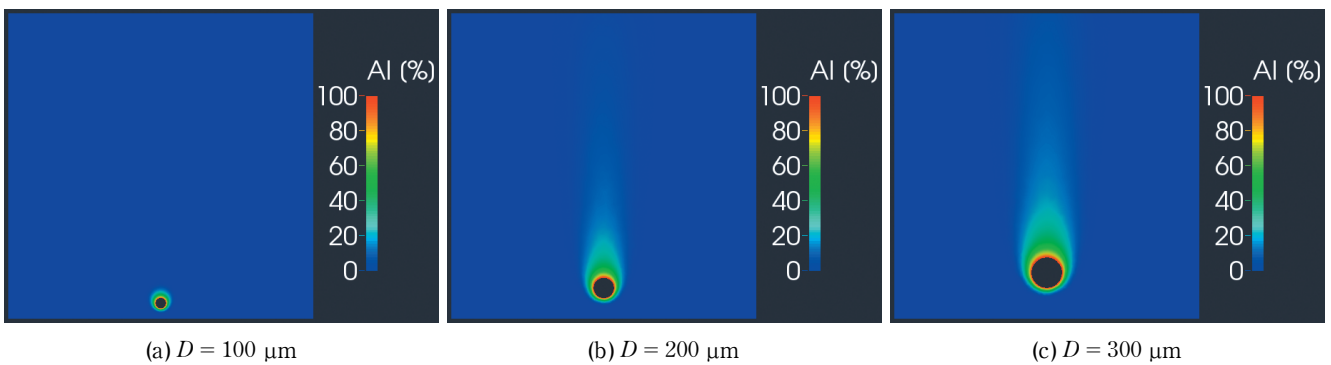


Figure 3 Concentration distributions of vaporized aluminum, CO_2 , $U_g = 14 \text{ m s}^{-1}$.

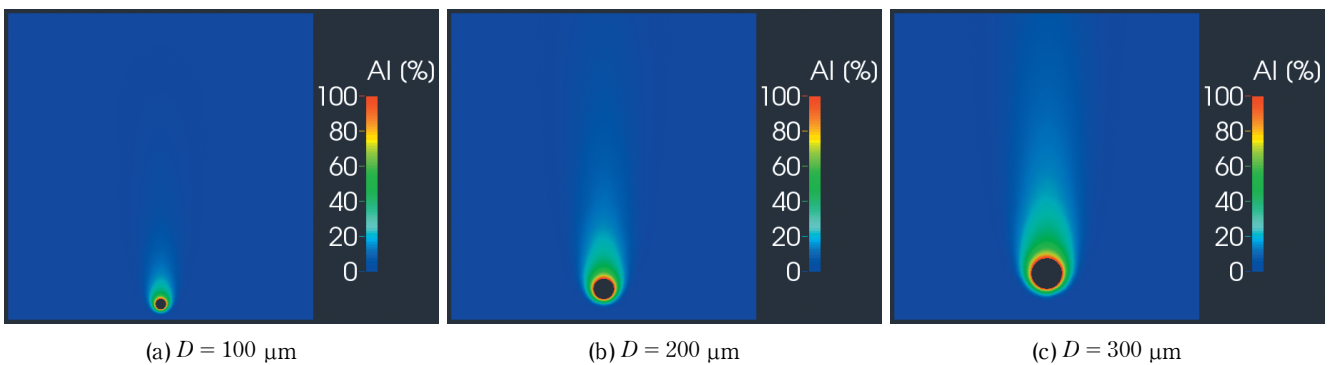


Figure 4 Concentration distributions of vaporized aluminum, H_2O , $U_g = 14 \text{ m s}^{-1}$.

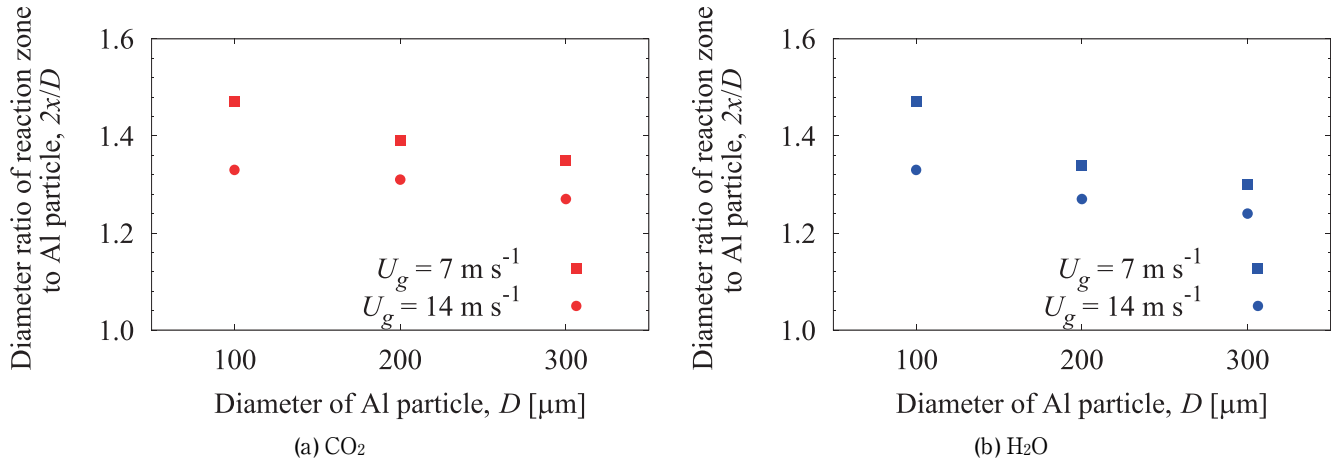


Figure 6 Diameters of reaction zone.

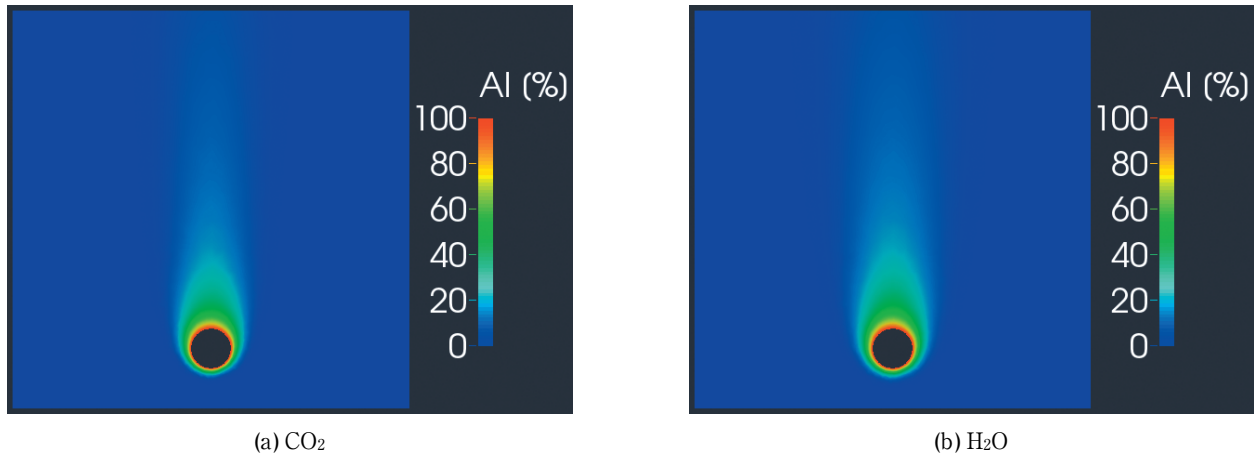


Figure 7 Influence of oxidizer on cloud of vaporized aluminum, $D = 300 \mu\text{m}$ $U_g = 14 \text{ m s}^{-1}$.

presented in Figure 6. The reaction zone diameters are indicated with changing aluminum particle diameter for the respective gas and the gas velocity. The reaction zone diameters are expressed with $2x$, where x is the distance from the center of aluminum particle to the reaction zone in Figures 3 and 4, and the direction of x is perpendicular to the gas flow direction, as shown in Figures 1 and 2.

The reaction zone diameter is about 1.2-1.5 D of the aluminum particle diameter. The reaction zone closes to the particle with increasing diameter. Therefore, it is considered that the luminous flame becomes closer to the aluminum particle with increasing diameter of the particle because the luminous flame occurs at the same location of the reaction zone. The luminous flame diameter is estimated as about 1.2-1.5 D from the reaction zone diameter. The influences of the oxidizer and the gas velocity will be described in later sections.

3.2 Influence of oxidizer

The concentration distributions of vaporized aluminum around the aluminum particle are presented in Figure 7 with comparison of oxidizers. As explained in Section 3.1, the figure is cross-section views of the computational domain. The aluminum particle diameter is $D = 300 \mu\text{m}$ on behalf of all the diameters.

As the figures show, the vaporized aluminum cloud in CO_2 is slightly narrower than that in H_2O , but the difference by the oxidizer is extremely small. However, as

shown in the case of $D = 100 \mu\text{m}$ in Figures 3 and 4, when the diameter is small, the difference by the oxidizer appears on the shapes of vaporized aluminum clouds. The oxidizer viscosity is considered to affect the gas flow around the small diameter particle such as $D = 100 \mu\text{m}$. Therefore, the cloud shape is different.

3.3 Influence of gas velocity

The concentration distributions of vaporized aluminum around the aluminum particle are presented in Figure 8 with comparison of gas velocities. As explained in Section 3.1, the figure is cross-section views of the computational domain. The aluminum particle diameter is $D = 200 \mu\text{m}$ on behalf of all the diameters.

In this study, the heterogeneous decomposed gas velocity is simulated with changing gas velocity. The shape of the vaporized aluminum cloud is slightly narrower with increasing gas velocity. The difference of the reaction zone diameter is about 0.1-0.2 D , as shown in Figure 6. Thus, the difference by the gas velocities is very small.

To examine the shape of the vaporized aluminum cloud, it is necessary to investigate the gas flow around the aluminum particle. The distributions of gas velocity are presented in Figure 9 corresponding to Figure 8.

The low velocity area appears at the same location as the vaporized aluminum cloud. Thus, the low velocity area makes the vaporized aluminum clouds. As same in Figure

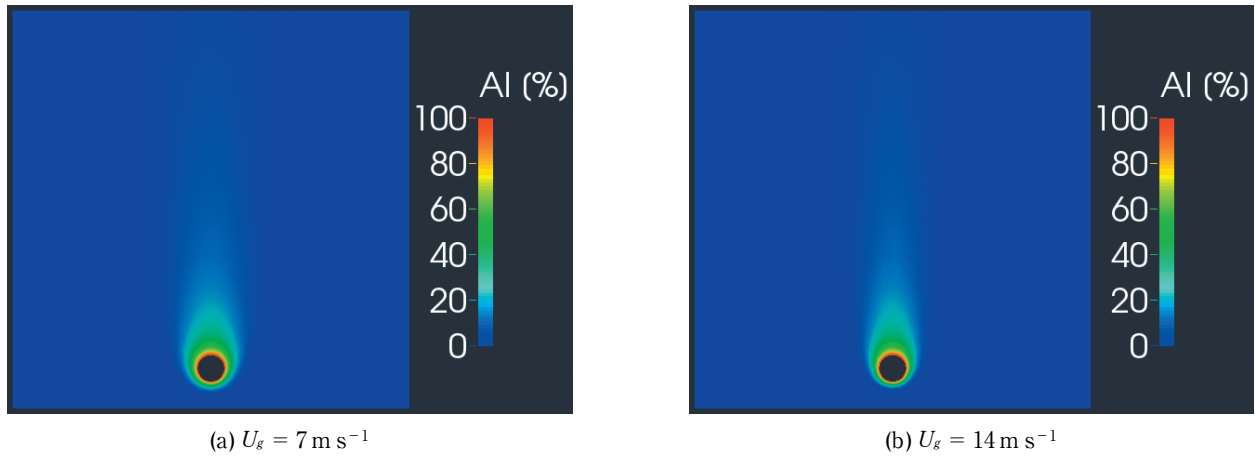


Figure 8 Influence of gas velocity on cloud of vaporized aluminum, $D = 200\mu\text{m}$, CO_2 .

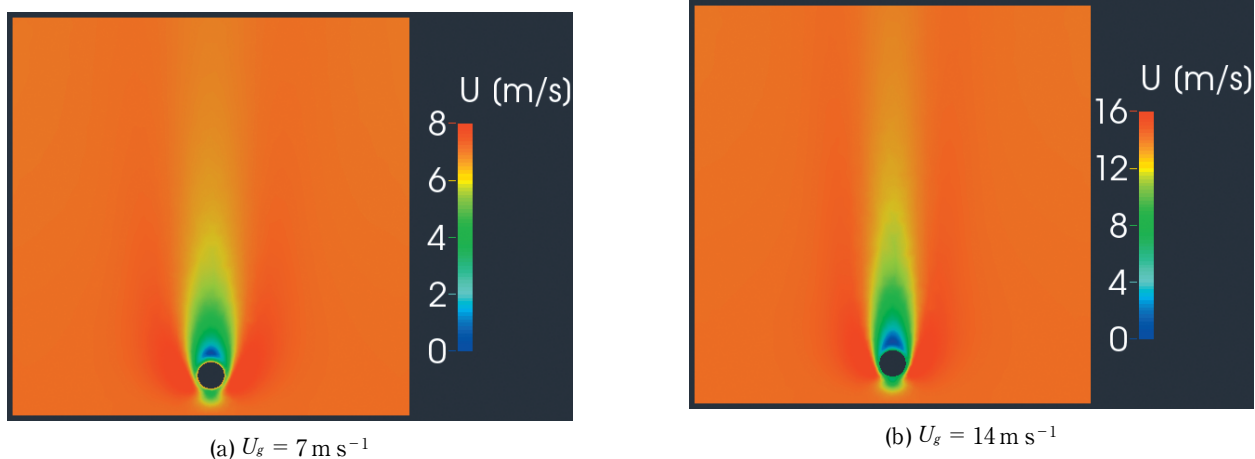


Figure 9 Distribution of gas velocity, $D = 200\mu\text{m}$, CO_2 .

8, the difference by the gas velocities is very small.

In earlier studies, the gas flow around the aluminum particle is regarded as Stokes flow^{1), 2), 18)}. However, the wake appears in the downstream of the particle. The cloud spreads mainly in the low-velocity area. The gas velocity distribution affects the cloud shape. The cloud shape resembles a raindrop because the low-velocity area spreads in the downstream of the aluminum particle, as shown in Figure 9.

3.4 Influence of the vaporized aluminum velocity

The concentration distributions of vaporized aluminum around the aluminum particle are presented in Figure 10 with comparison of velocities of vaporized aluminum. As explained in Section 3.1, the figure is cross-section views of the computational domain. The aluminum particle diameter is $D = 200\mu\text{m}$ on behalf of all the diameters.

As Figure 1 shows, the vaporized aluminum velocity is affected because there is alumina cap or alumina on the surface of melted aluminum. To simulate the influence of the aluminum particle surface, the vaporized aluminum velocity was varied in $U_{Al} = 3.4, 6.8, 13.6 \text{ m s}^{-1}$.

As shown in Figure 10, the vaporized aluminum cloud shape narrows with increasing vapor velocity. Because the gas velocity around the aluminum particle increases concomitantly with increasing vaporized aluminum velocity, the low-velocity area around the particle decreases. Therefore, the cloud is narrower.

To examine the vaporized aluminum cloud shape, the reaction zone diameters are presented in Figure 11 with varying velocities of vaporized aluminum. The reaction zone diameters are measured in the same way as Section 3.1, and they are indicated for the respective gas.

The reaction zone diameter decreases with increasing vapor velocity. The reaction zone closes to the aluminum particle surface with increasing vapor velocity. Therefore, it is considered that the luminous flame diameter decreases concomitantly with increasing vapor velocity because the luminous flame occurs at the same location of the reaction zone.

3.5 Evaluation of numerical experiments

In this study, the luminous flame diameters were estimated from numerical experiments. The diameters were obtained theoretically from the vaporized aluminum cloud around the aluminum particle. As Figure 12 shows, the study results are compared with the experimentally obtained results presented in our previous works^{9), 10)}. The numerical results are the same as the case of $U_g = 14 \text{ m s}^{-1}$ in Figure 6.

The numerical results are slightly smaller than the experimentally obtained results. In this study, we didn't calculate the chemical reactions. Therefore, these slight differences occurred near the location of the reaction zone because the chemical reactions occur at the reaction zone mainly. However, the numerical results closely

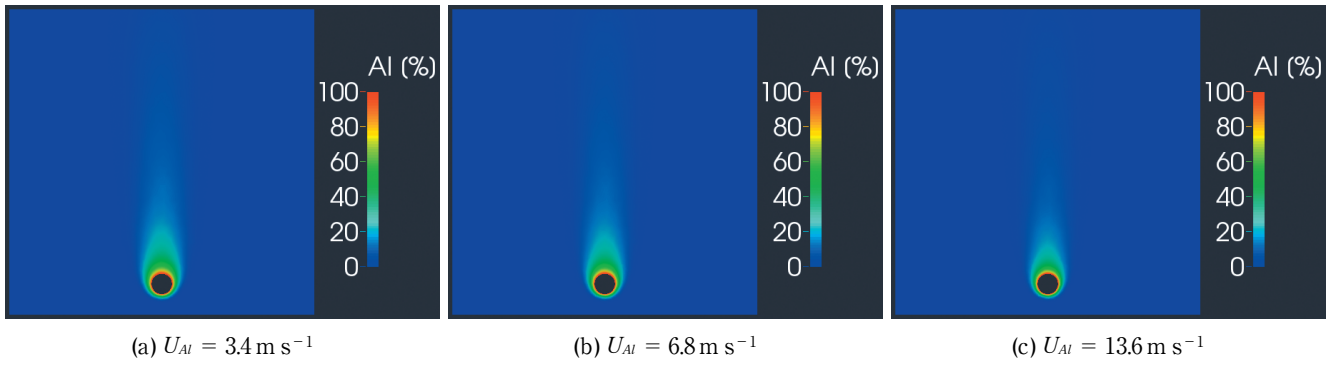


Figure 10 Influence of velocity of vaporized aluminum, $D = 200\mu\text{m}$, CO_2 , $U_g = 14\text{ m s}^{-1}$.

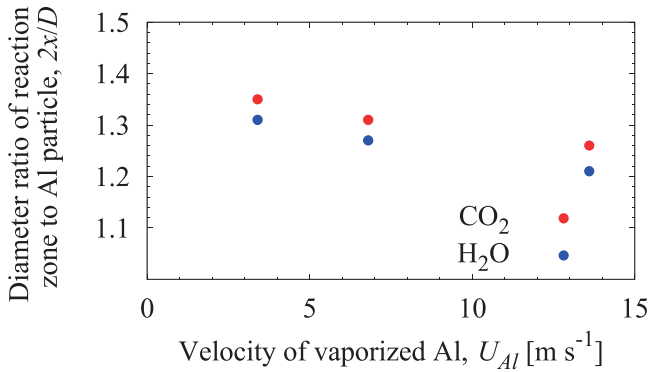


Figure 11 Diameters of reaction zone with varying velocity of vaporized aluminum.

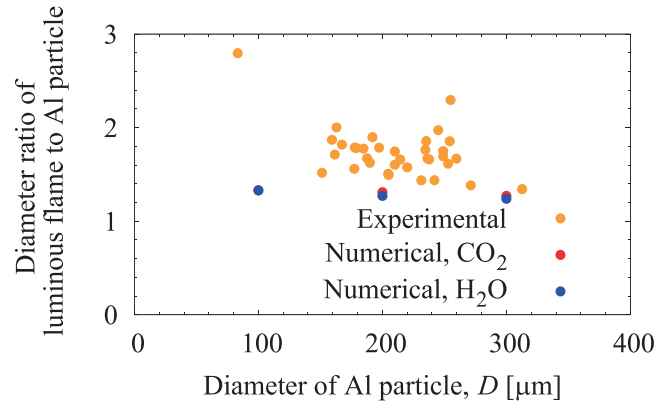


Figure 12 Luminous flame diameter, numerical vs. experimental.

approximate the experimentally obtained results. Consequently, the estimation method of this study is almost suitable.

4. Conclusion

The cloud of vaporized aluminum ejected from the aluminum particle surface spread around the particle. Results show that the cloud shape was streamlined, resembling a raindrop. The cloud shape changed by the gas velocity and the vaporized aluminum velocity. The cloud area decreased with increasing gas velocity and vaporized aluminum velocity. The numerically estimated luminous flame diameters are slightly smaller than the experimentally obtained results of our previous works.

Acknowledgement

This work was sponsored by the Foundation for the Promotion of Industrial Explosives Technology 2011-2014.

References

- 1) K. Kuo and M. Summerfield, "Fundamentals of Solid-Propellant Combustion," *Prog. Astronaut. Aeronaut.*, 90 (1984).
- 2) V. Yang, T. B. Brill, and W-Z. Ren, "Solid Propellant Chemistry, Combustion, and Motor Interior Ballistics," *Prog. Astronaut. Aeronaut.*, 185 (2000).
- 3) N. Kubota, "Propellants and Explosives: Thermochemical Aspects of Combustion, Second Rev. Exp.," Wiley-VCH Verlag GmbH & Co. KGaA (2007).
- 4) Propellant committee, "Propellant Handbook," Japan Explosives Society (2005).
- 5) S. Oide, K. Takahashi, and T. Kuwahara, 48th AIAA/ASME/SAE/ASEE Joint Propulsion Conference, AIAA Paper 2012-3973 (2012).
- 6) S. Oide, K. Takahashi, and T. Kuwahara, *Sci. and Tech. Energetic Materials*, 73, 153-156 (2012).
- 7) K. Takahashi, S. Oide, M. Tanabe, T. Kuwahara, and T. Shimada, *Proceedings of Autumn Meeting of Japan Explosive Society*, 51-54 (2012) (in Japanese).
- 8) K. Takahashi, S. Oide, and T. Kuwahara, *Propellants, Explosives, Pyrotechnics*, 38, 555-562 (2013).
- 9) T. Kuwahara, S. Sakai, R. Doi, T. Sasaki, and K. Takahashi, *Proceedings of Autumn Meeting of Japan Explosive Society*, 9 (2013) (in Japanese).
- 10) R. Doi, K. Takahashi, and T. Kuwahara, *Proceedings of Spring Meeting of Japan Explosive Society*, 79-80 (2014) (in Japanese).
- 11) M. W. Beckstead, *RTO/VKI Special Course on Internal Aerodynamics in Solid Rocket Propulsion*, RTO-EN-023 (2004).
- 12) V. E. Zarko and O. G. Glotov, *Sci. and Tech. Energetic Materials*, 74, 139-143 (2013).
- 13) O. Orlandi and Y. Fabignon, 37th AIAA/ASME/SAE/ASEE Joint Propulsion Conference, AIAA Paper 2001-3582 (2001).
- 14) E. B. Washburn, M. L. Gross, S. T. Smith, and S. Balachandar, 46th AIAA/ASME/SAE/ASEE Joint Propulsion Conference, AIAA Paper 2010-6677 (2010).
- 15) E. B. Washburn, J. A. Webb, and M. W. Beckstead, *Combust. Flame*, 157, 540-545 (2010).
- 16) B. T. Bojko, P. E. DesJardin, and E. B. Washburn, *Combust. Flame*, in Press (2014).
- 17) S. Gordon and B. J. McBride, *NASA Reference Publication*, NASA RP-1311 (1994).
- 18) C. T. Crowe, J. D. Schwarzkopf, M. Sommerfeld, and Y. Tsuji, "Multiphase Flows with Droplets and Particles Second Ed.," CRC Press (2012).